

Supporting Information

Synergistic interplay of Zn and Rh-Cr promoters on Ga₂O₃ based photocatalyst for water splitting

Marta Borges Ordoño^a, Shunsaku Yasumura^a, Pieter Glatzel^b,

and Atsushi Urakawa^{*a}

^a*Institute of Chemical Research of Catalonia (ICIQ), The Barcelona Institute of Science and
Technology, Tarragona, 43007, Spain*

^b*ESRF - The European Synchrotron, Grenoble, 38043, France*

**E-mail: aurakawa@iciq.es*

MATERIALS CHARACTERIZATION

UV-Vis DRS measurements were performed on a Shimadzu UV-2401PC spectrophotometer with D₂ and W lamps as light sources, and a photomultiplier detector. Solid samples were introduced in a round holder with a fused silica window on an integrating sphere attachment ISR-240A from Shimadzu. BaSO₄ was used as internal standard and spectra were collected between 240 and 800 nm. Band gap (E_g) was calculated from the slope intersection of the normalized Kubelka-Munk absorption spectrum.

Scanning transmission electron microscopy (STEM) was measured in annular dark-field imaging mode (HAADF) in a high-resolution FEI Tecnai F20 STEM microscope at ICN2 (Barcelona). Chemical analysis and chemical mapping were performed by energy dispersive X-ray spectroscopy (EDX) and electron energy loss spectroscopy (EELS), respectively. 4 wt% Zn-Ga₂O₃ and Rh-Cr/4wt% Zn-Ga₂O₃ materials prepared in ethanol solution and were deposited on the a TEM support grid.

Cr and Rh elements were studied at their corresponding K-edge energies 5.99 and 23.22 keV, respectively. HERFD-XANES were measured from 5.98 to 6.08 keV (Cr) and 23.18 to 23.40 keV (Rh); with a step size for Cr of 0.1 eV and 0.05 eV for Rh. The spectrometer was equipped with four spherical Ge (333) crystal for Cr, and a diode IF3 with Cu+Ni filter was used for Rh detection. All the samples and reference materials were measured ex situ in the form of pellet (13 mm diameter), containing 60 mg of material and 60 mg of cellulose.

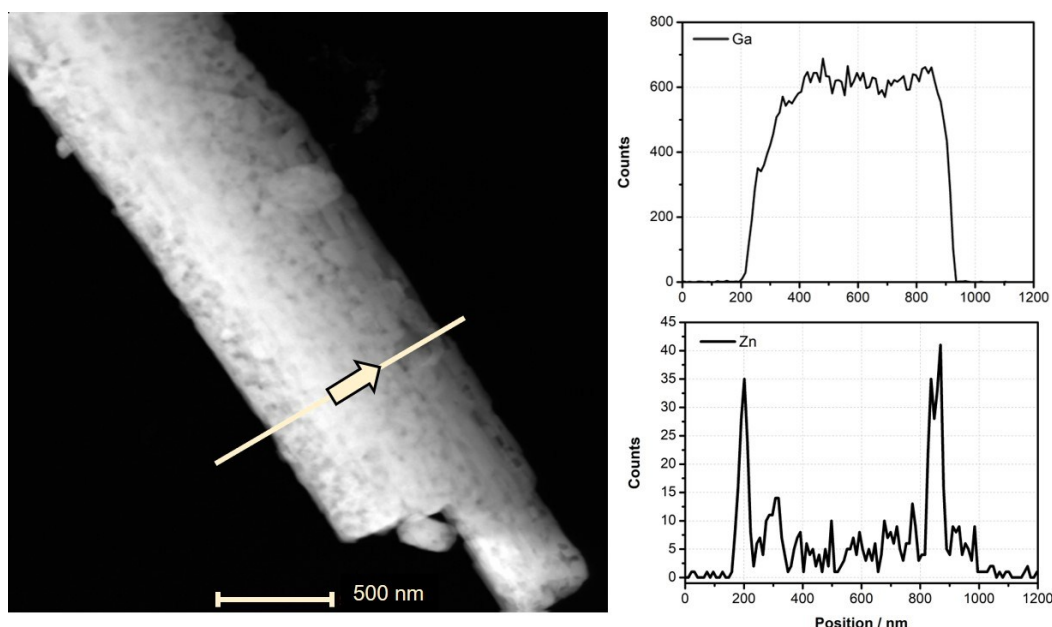


Fig. S1 (left) STEM-HAADF image of 4 wt% Zn-Ga₂O₃ material, with the transversal line indicating where EDX was measured. (right) Elemental profiles of Ga (top) and Zn (bottom) along the transversal line.

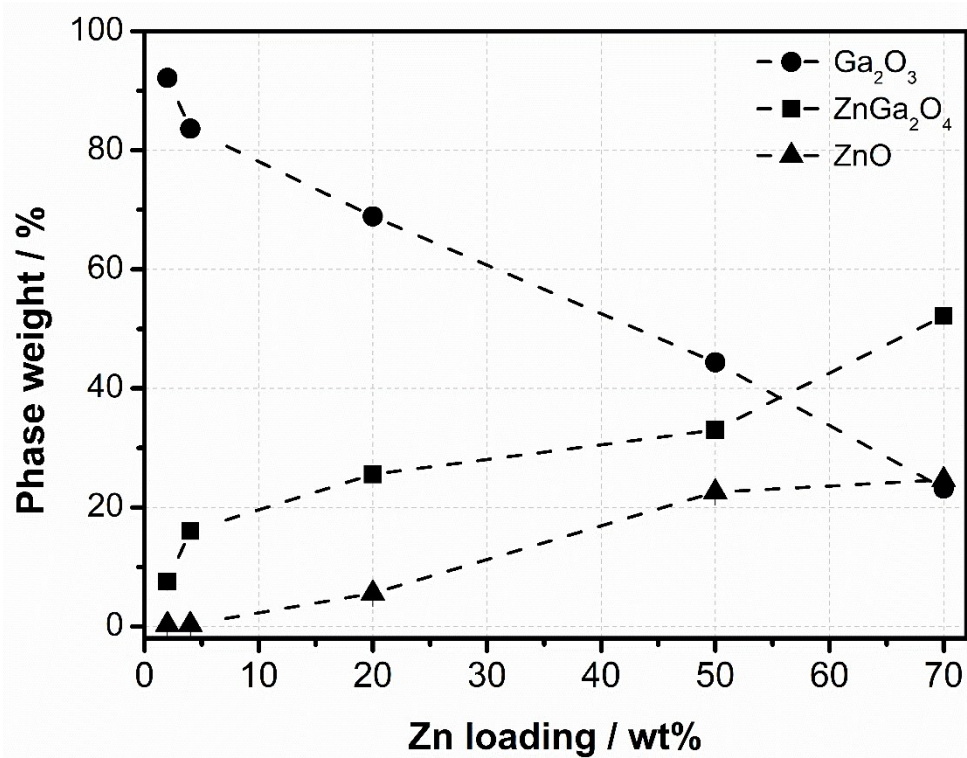


Fig. S2 Quantitative phase analysis of the XRD data for xZn-modified Ga₂O₃ photocatalysts where x= 2, 4, 20, 50, and 70 wt% of Zn.

Table. S1 Relative shift calculated from K β lines using the center of mass for Zn-Kedge (top) and Ga-Kedge (bottom).

Sample	K β	Center of mass (eV)	Relative shift (eV)
ZnO	1	9571.863	0
	2	9571.863	
ZnGa ₂ O ₄	1	9571.832	0
	2	9571.832	
2 wt% Zn-Ga ₂ O ₃	1	9571.842	0.002
	2	9571.844	
4 wt% Zn-Ga ₂ O ₃	1	9571.842	0
	2	9571.842	
20 wt% Zn-Ga ₂ O ₃	1	9571.855	0.003
	2	9571.852	
50 wt% Zn-Ga ₂ O ₃	1	9571.854	0.005
	2	9571.859	
70 wt% Zn-Ga ₂ O ₃	1	9571.853	0.001
	2	9571.854	

Sample	K β	Center of mass (eV)	Relative shift (eV)
Ga ₂ O ₃	1	10264.09	0
	2	10264.09	
ZnGa ₂ O ₄	1	10264.07	0
	2	10264.07	
2 wt% Zn-Ga ₂ O ₃	1	10264.11	0.01
	2	10264.12	
4 wt% Zn-Ga ₂ O ₃	1	10264.11	0
	2	10264.11	
20 wt% Zn-Ga ₂ O ₃	1	10264.13	0
	2	10264.13	
50 wt% Zn-Ga ₂ O ₃	1	10264.12	0.01
	2	10264.13	
70 wt% Zn-Ga ₂ O ₃	1	10264.06	0
	2	10264.06	

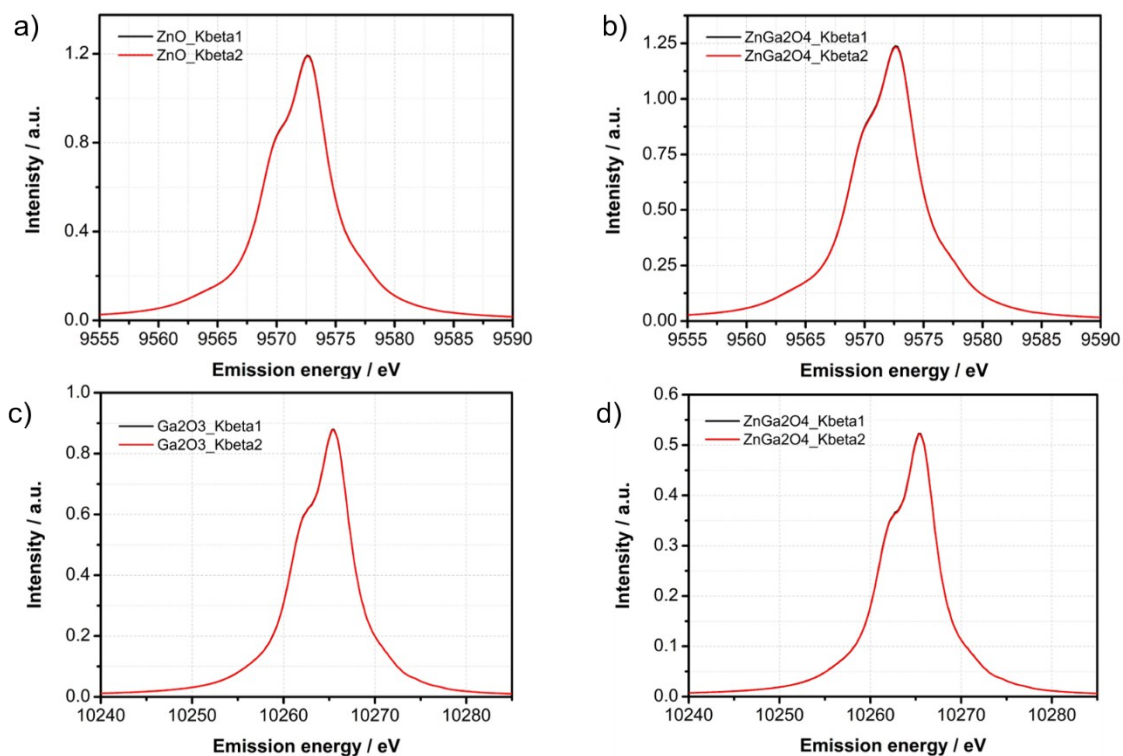


Fig. S3 Comparison of successive scans of K β main line for Zn K-edge a) ZnO and b) ZnGa₂O₄ and Ga K-edge c) Ga₂O₃ and d) ZnGa₂O₄.

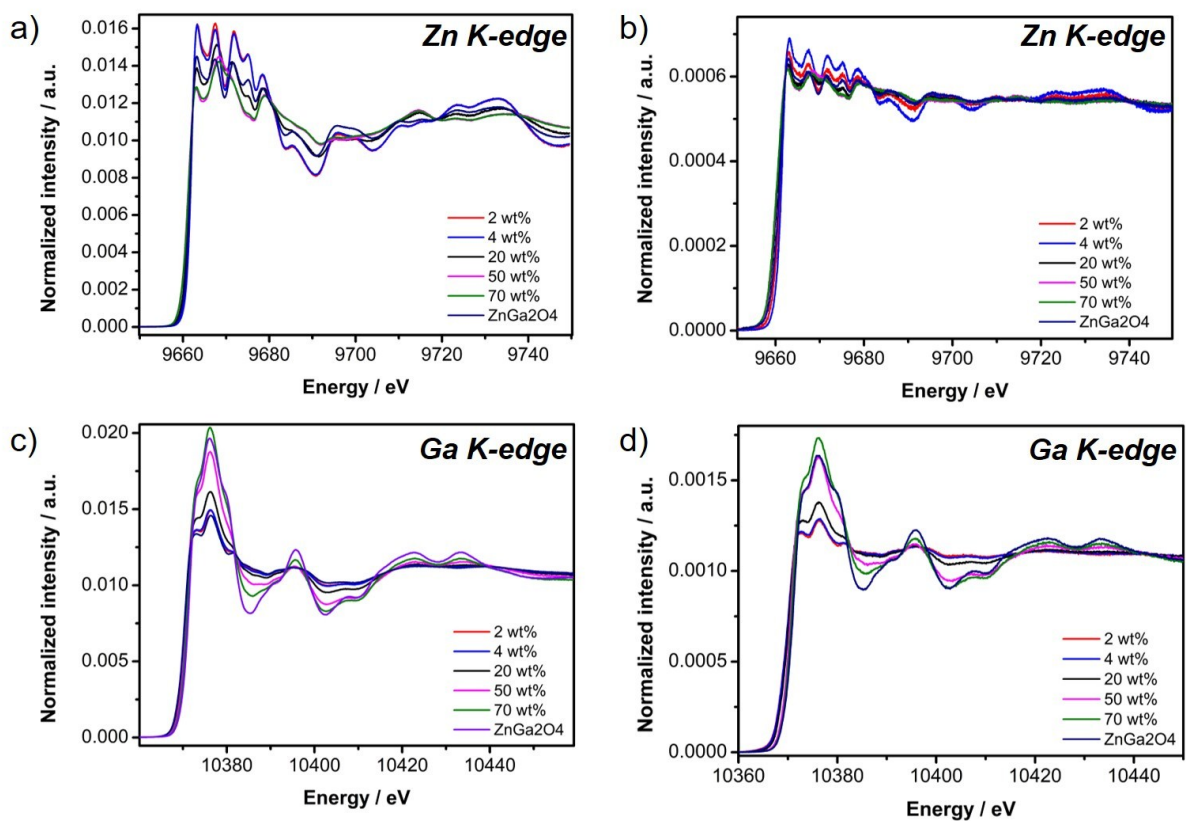


Fig. S4 XANES for Zn K-edge and Ga K-edge comparing HERFD scans (a and c) with total fluorescence scans (b and d).

The performance of density functionals PBE and PBE0 was compared, but due to the high computational cost of PBE0, PBE was applied to perform the cell optimization of the ZnO, Ga₂O₃, and ZnGa₂O₄ structures. First, the atomic positions in the corresponding cells and lattice parameters were optimized using PBE. After this, the energy calculations were performed by PBE0 to obtain more accurate DOS with the atomic positions and lattice parameters calculated above.

Table S2. DOS calculations details

Package			
	CASTEP		
Conditions of Cell optimization			
	ZnO	Ga ₂ O ₃	ZnGa ₂ O ₄
Functional	PBE	PBE	PBE
Energy tolerance (eV/atom)	1.00E-05	1.00E-05	1.00E-05
Max. force(eV/Å)	0.03	0.03	0.03
Max. stress (Gpa)	0.05	0.05	0.05
Max. displacement (Å)	0.001	0.001	0.001
Energy cutoff (eV)	750	800	800
K-mesh	5x5x4	5x5x2	3x3x3
SCF tolerance (eV/atom)	1.00E-06	1.00E-06	1.00E-06
Conditions of SCF by PBE0			
	ZnO	Ga ₂ O ₃	ZnGa ₂ O ₄
Functional	PBE0	PBE0	PBE0
Energy cutoff (eV)	600	600	600
K-mesh	4x4x2	4x4x2	3x3x3
SCF tolerance (eV/atom)	2.00E-06	2.00E-06	2.00E-06

The coverage or phase transformation of ZnGa₂O₄ into ZnO could be further determined by looking deeper into the Zn K-edge VtC-XES region. Typically, VtC spectra has two lines corresponding to $K\beta_{2,5}$ (located below the Fermi level) and $K\beta''$ (cross over) at lower fluorescence energy.¹ At low Zn concentrations (2 and 4 wt%) the $K\beta''$ line was split because of the interaction from the metal (Zn) with s orbitals of O and d orbitals of Ga (**Fig. S5**), this result was supported by the density of states calculations on the reference materials (details of calculation shown in **Table S2**). On the contrary, at high Zn loadings where ZnO phase was detected the $K\beta''$ line only contains the contribution of s orbitals from O, indicating that first coordination shell of Zn atoms does not contain Ga atoms which might be attributed to the reduced accessibility of Zn atoms to the Ga₂O₃ surface, in agreement with the EXAFS analysis (**Fig. S6**). In addition, the third emission line due to multielectron transitions (ME) from the emitted and absorbed photoelectrons is observed in the Zn K-edge VtC spectra (**Fig. S5**). The intensity of this ME region is located above the Zn absorption edge energy and decreases with

ZnO formation following the same trend that the photocatalytic activity results. However, correlation with the catalytic results are not discussed here because of the self-absorption effects that could also contribute to the ME intensity.^{2,3}

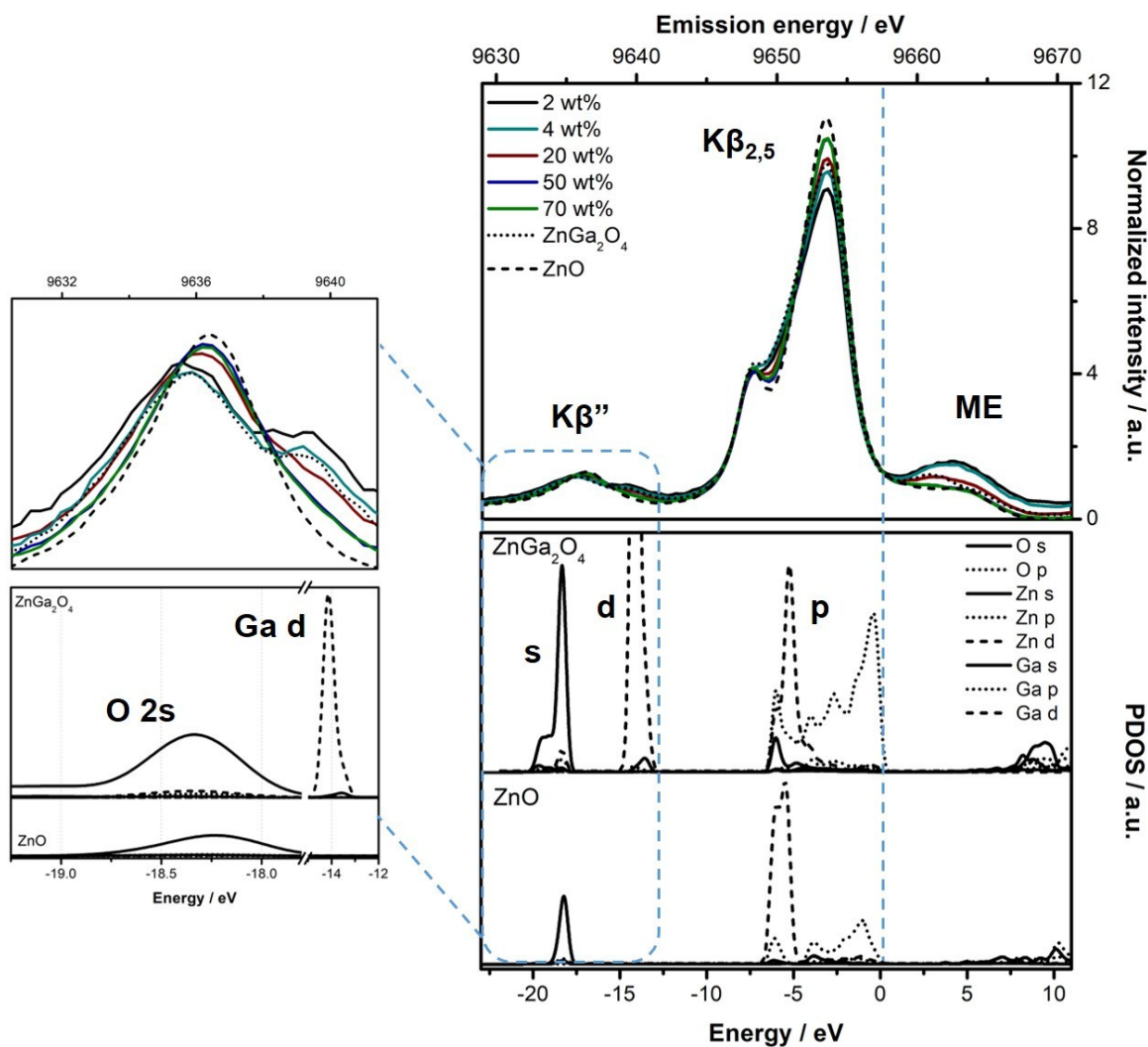


Fig. S5 Zn K-edge VtC-XES with normalized intensity to the spectral area (top). PDOS calculations for O, Ga, and Zn where mainly s and p regions correspond to the Kβ'' and Kβ_{2,5} lines, respectively. The dashed blue line indicates the Fermi level, and the zoomed region corresponds to Kβ''.

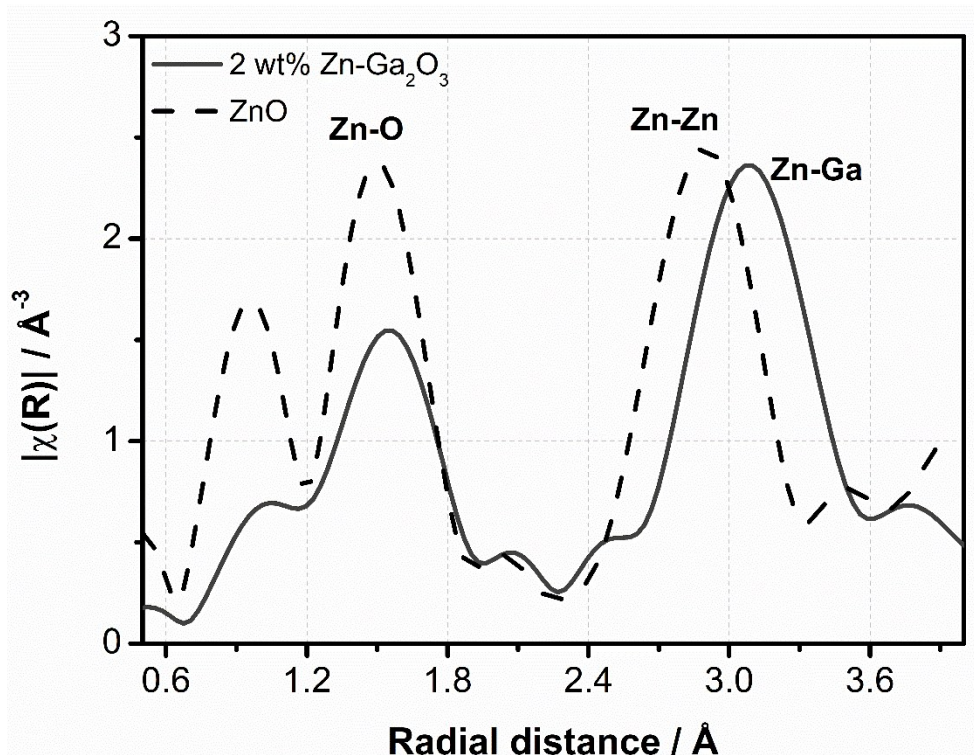


Fig. S6 EXAFS analysis of low Zn content Ga_2O_3 (2 wt%) compared to ZnO (dotted line) reference material. Self-absorption correction was performed on the ZnO EXAFS data by using the Fluo algorithm (Haskel, 1999).

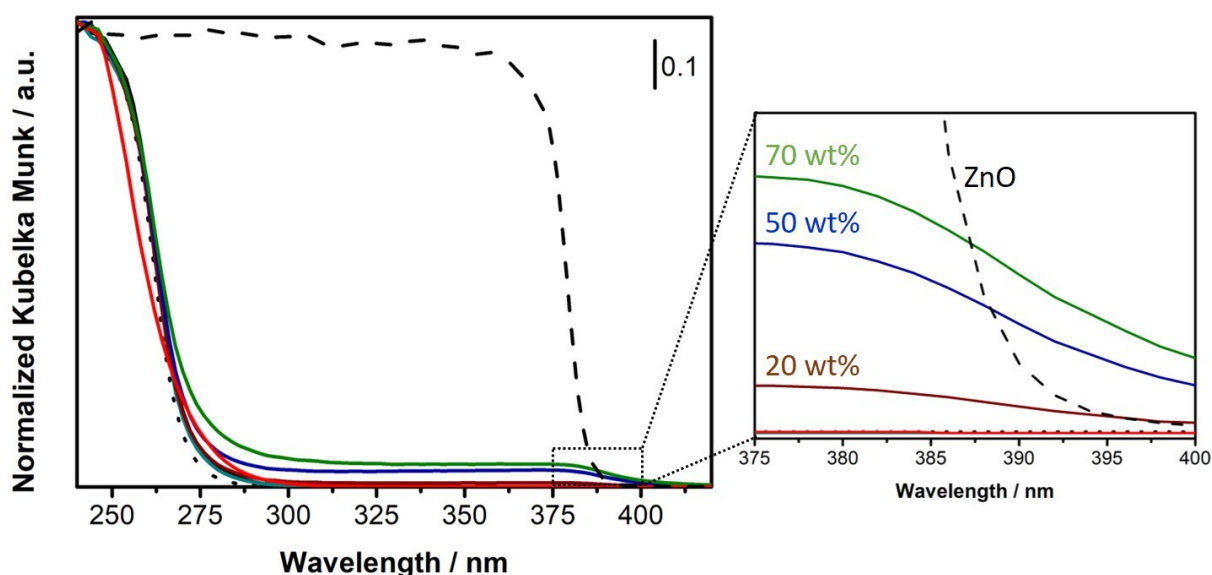


Fig. S7 UV-Vis DR spectra of $x\text{Zn-Ga}_2\text{O}_3$ materials with $x = 2$ (black), 4 (cyan), 20 (maroon), 50 (blue) and 70 (green) and of reference materials, ZnGa_2O_4 (red), Ga_2O_3 (dotted line) and ZnO (dashed line). Spectra are shown in normalized Kubelka-Munk absorbance unit and the bandgaps were calculated from the slope of the adsorption spectra. Zoomed plot shows the region highlighting light absorption by ZnO.

For both Zn K-edge (**Fig. S8a**) and at Ga K-edge (**Fig. S8b**), opposite trends are observed for the unoccupied energy levels at the Zn and Ga absorption edges (inset plots, **Fig. S8**). For the Zn K-edge, at small Zn concentrations (2 and 4 wt%) the lowest-unoccupied electronic states appear to be comparable to those of ZnGa_2O_4 (**Fig. S8a**), while at increasing Zn-loading where ZnO phase is more prominent, the absorption edges shift to lower energies, corresponding to smaller valence-conduction band gaps. This agrees with the UV-Vis DRS study (**Fig. S7**), at high Zn loading (≥ 20 wt%) a weak absorption extending in the visible region appears clearly due to the presence of ZnO, with the optical bandgap of 3.0-3.1 eV.

In contrast, the lowest-unoccupied energy states of Ga are shifted toward higher energies at higher Zn content, pure ZnGa_2O_4 shows the highest lowest-unoccupied energy state (**Fig. S8b**). The small shift of the unoccupied energy states of Ga at low Zn concentrations (e.g. energy difference between Ga_2O_3 and 4 wt% Zn- Ga_2O_3 is 0.06 eV) is likely attributed to the minor contribution of ZnGa_2O_4 phase for such Zn loadings.

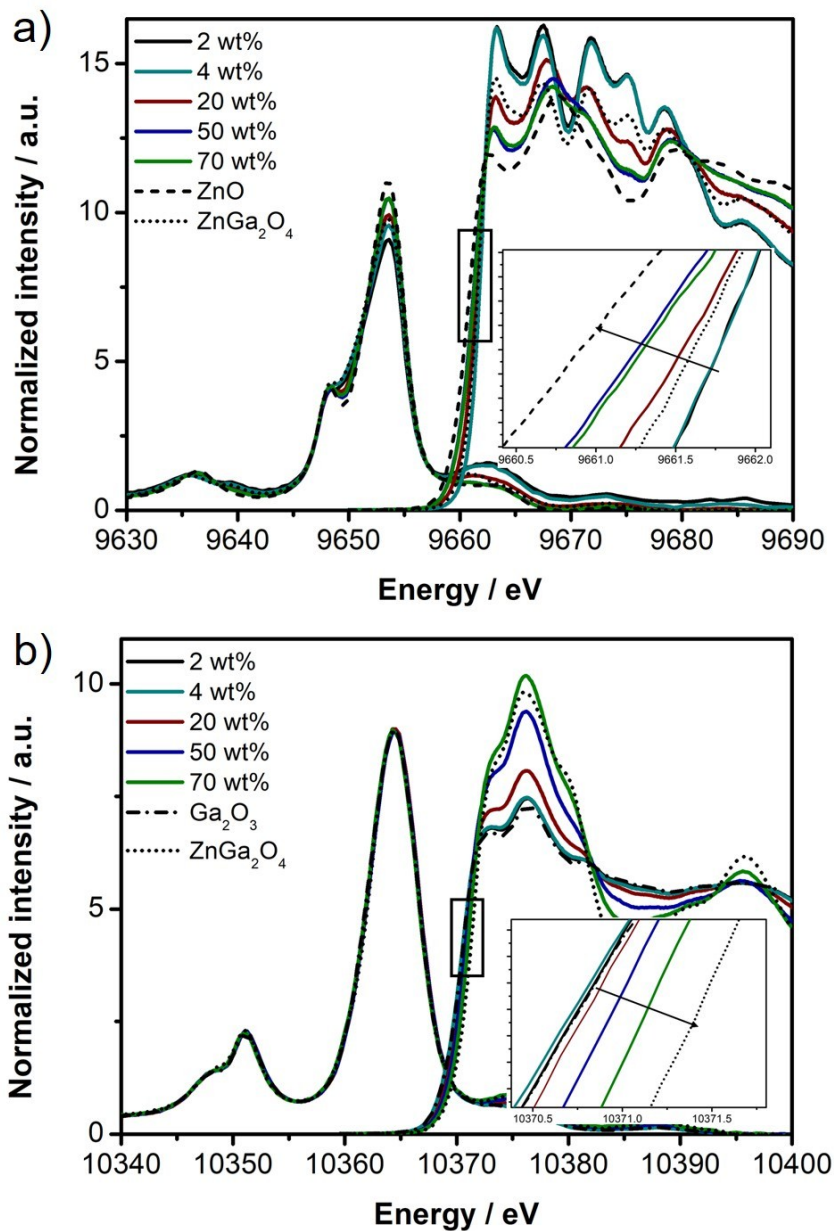


Fig. S8 XAS and VtC-XES spectra for a) Zn K-edge and b) Ga K-edge. Pure ZnGa₂O₄ (dotted line), ZnO (dashed line), and Ga₂O₃ (dot-dashed line). Spectral intensity was normalized to the spectral area. Inset figures show the opposite energy changes of the absorption edge.

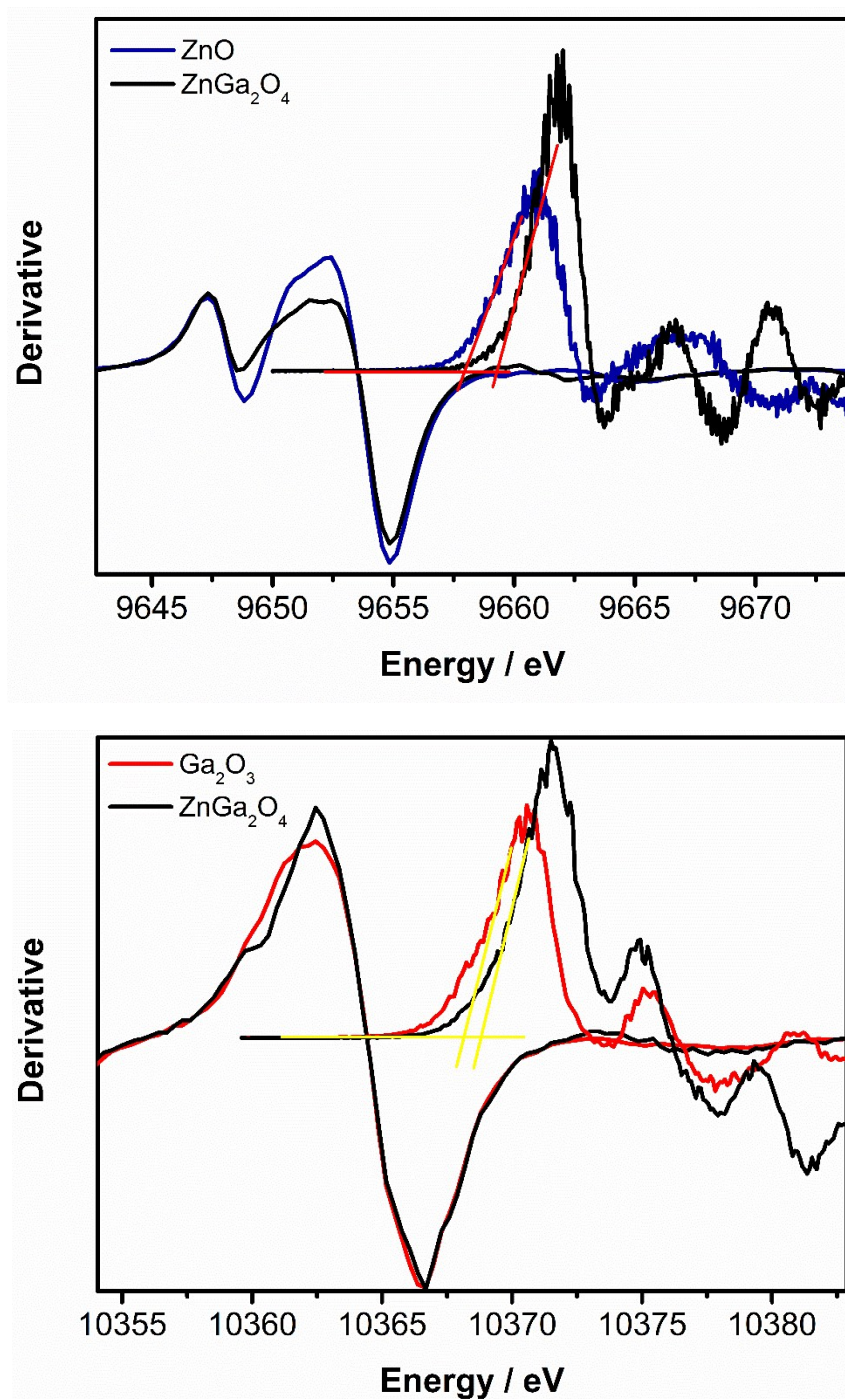


Fig. S9 First derivative of XAS and VtC-XES spectra for Zn K-edge (top) and Ga K-edge (bottom). Red and yellow lines are positioned at the intersection between baseline at 0 intensity and the slope of the first derivative of XAS, and the intersection from the baseline for XAS and XES was used to calculate the difference between the XAS and XES spectra.

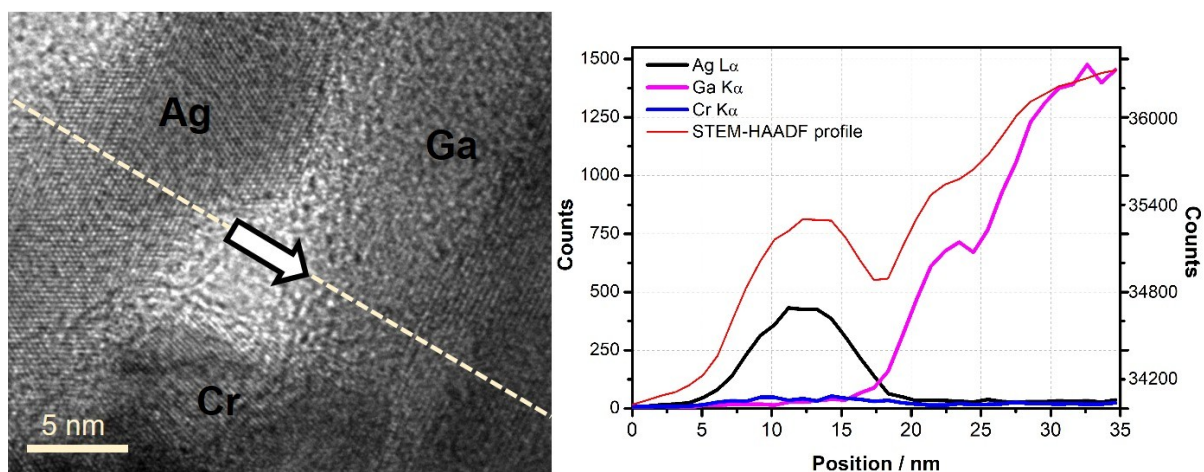


Fig. S10 STEM-HAADF image of Rh-Cr/4 wt% Zn-Ga₂O₃, and elemental profiles over the diagonal for Ag (black), Cr (blue), and Ga (pink). Rh was not detected likely due to its low content.

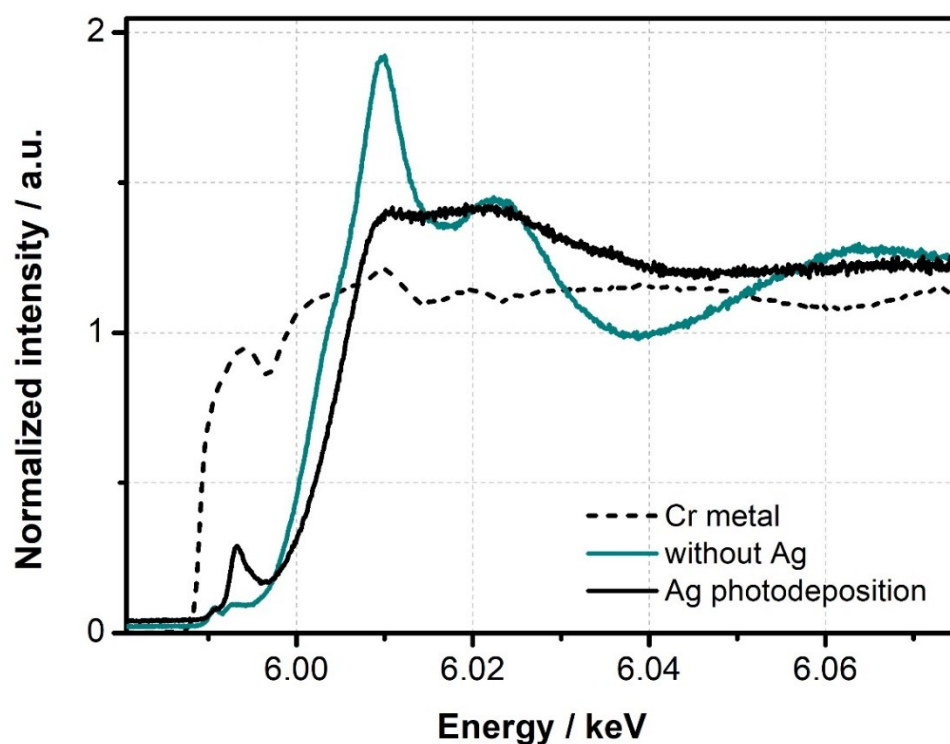


Fig. S11 XANES spectra at Cr K-edge; Cr metal (dashed line), Rh-Cr/4 wt% Zn-Ga₂O₃ (cyan), and after silver photodeposition (black).

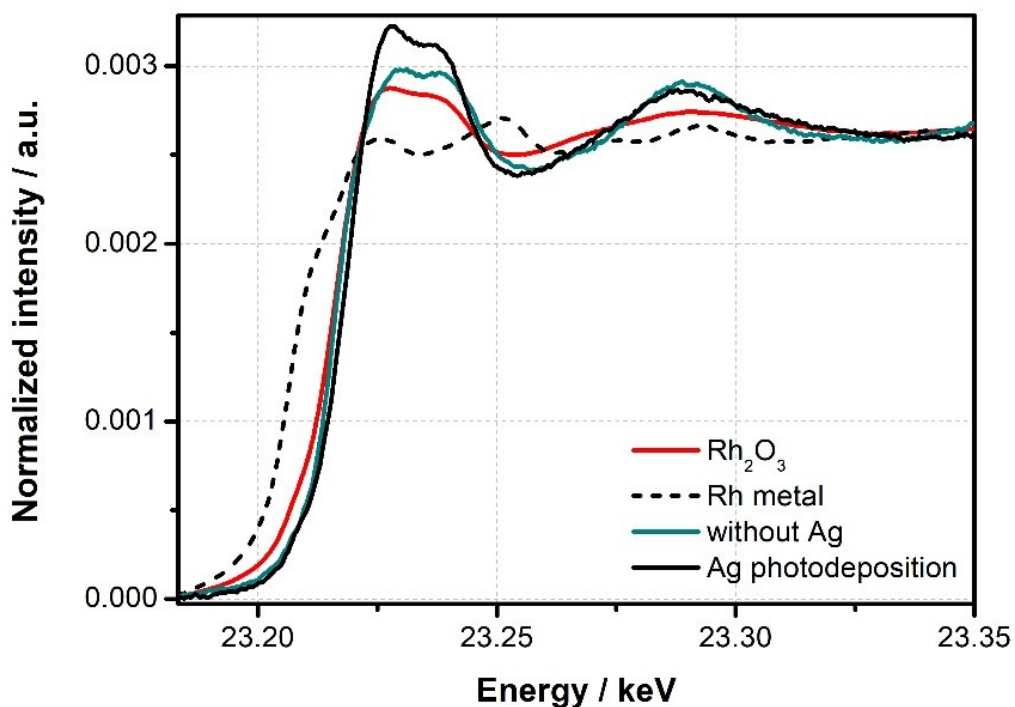


Fig. S12 XANES spectra at Rh K-edge; Rh-Cr/4 wt% Zn-Ga₂O₃ (cyan), and after silver photodeposition (black). Rh₂O₃ (red) and metallic Rh (dashed lines) were used as reference materials.

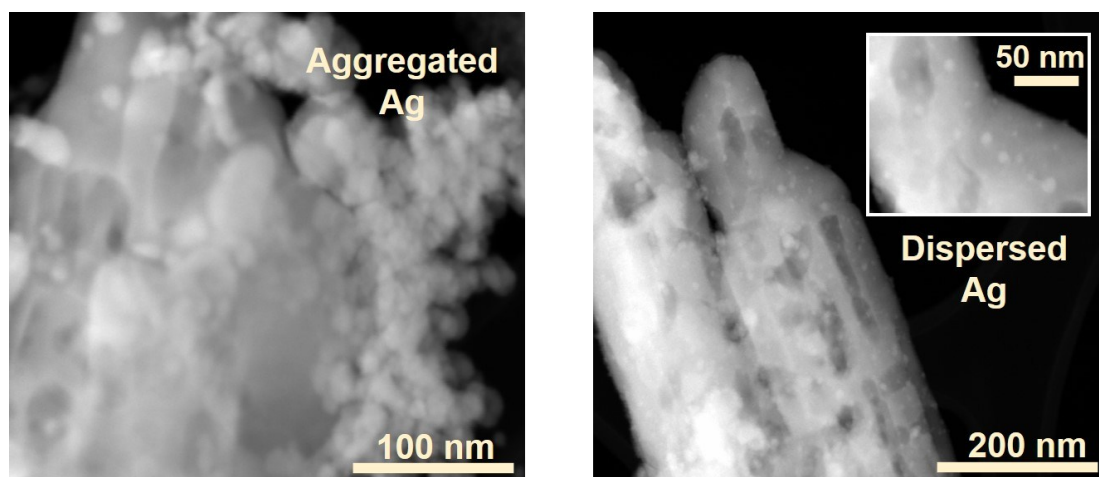


Fig. S13 STEM-HAADF images of 20 wt% Ag deposited on Rh-Cr/4wt% Zn-Ga₂O₃ after photodeposition (left) and after impregnation (right).

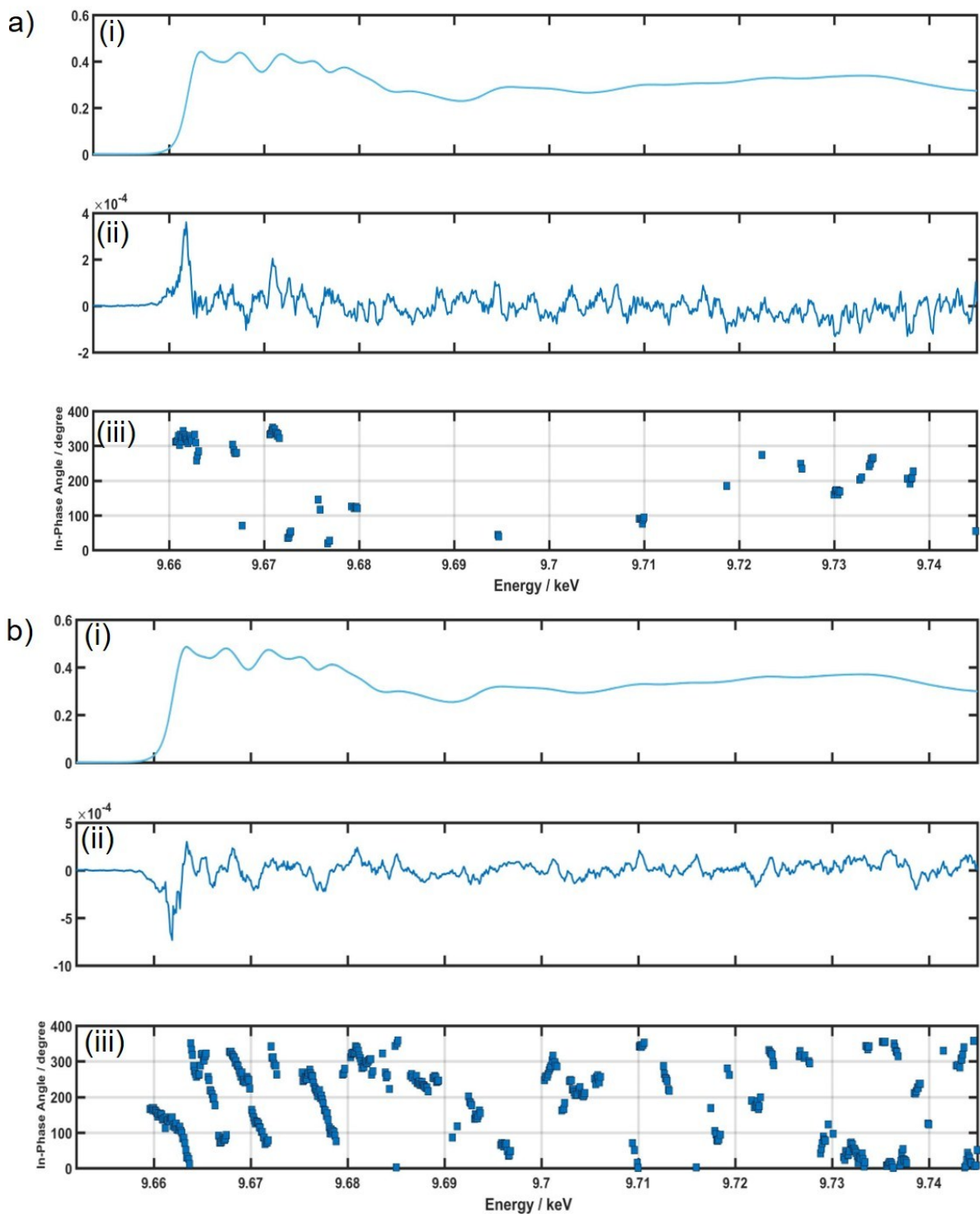


Fig. S14 Zn-Kedge HERDF-XANES phase-domain spectra and in-phase angles analysis for a) 4wt% Zn-Ga₂O₃ and b) Rh-Cr/4wt% Zn-Ga₂O₃. The amplitude threshold to plot the in-phase angles was 0.0001.

References

1. U. Bergmann, C. R. Horne, T. J. Collins, J. M. Workman and S. P. Cramer, *Chem. Phys. Lett.*, 1999, **302**, 119-124.
2. D. R. Mortensen, G. T. Seidler, J. J. Kas, N. Govind, C. P. Schwartz, S. Pemmaraju and D. G. Prendergast, *Phys. Rev. B.*, 2017, **96**, 125136.
3. R. A. Valenza, E. P. Jahrman, J. J. Kas and G. T. Seidler, *Phys. Rev. A.*, 2017, **96**, 032504.